

Impurity effects on the normal-state transport properties of $\text{Ba}_{0.5}\text{K}_{0.5}\text{Fe}_2\text{As}_2$ superconductors

Jun Li,^{1,2,*} Jie Yuan,^{3,2} Min Ji,^{2,4} Gufei Zhang,¹ Jun-Yi Ge,¹ Hai-Luke Feng,^{2,5} Ya-Hua Yuan,^{2,5} Takeshi Hatano,² Wei Hu,³ Kui Jin,³ Tobias Schwarz,⁶ Reinhold Kleiner,⁶ Dieter Koelle,⁶ Kazunari Yamaura,^{2,5} Hua-Bing Wang,^{2,4} Pei-Heng Wu,⁴ Eiji Takayama-Muromachi,^{7,5} Johan Vanacken,¹ and Victor V. Moshchalkov^{1,†}

¹INPAC - Institute for Nanoscale Physics and Chemistry, KU Leuven, Celestijnenlaan 200D, B-3001 Leuven, Belgium

²Superconducting Property Unit, National Institute for Materials Science, 1-1 Namiki, Tsukuba, Ibaraki 305-0044, Japan

³Condensed Matter Physics, Institute of Physics, Chinese Academy of Sciences, Beijing 100190, China

⁴Research Institute of Superconductor Electronics, Nanjing University, Nanjing 210093, China

⁵Graduate School of Chemical Sciences and Engineering, Hokkaido University, Sapporo, Hokkaido 060-0810, Japan

⁶Physikalisches Institut-Experimentalphysik II and Center for Collective Quantum Phenomena in LISA⁺, Universität Tübingen, Auf der Morgenstelle 14, D-72076 Tübingen, Germany

⁷International Center for Materials Nanoarchitectonics (WPI-MANA), National Institute for Materials Science, 1-1 Namiki, Tsukuba, Ibaraki 305-0044, Japan

(Received 30 April 2014; revised manuscript received 25 June 2014; published 14 July 2014)

We investigated the normal-state resistivity $\rho_{xx}(T)$ and the Hall effect in Zn- and Co-doped $\text{Ba}_{0.5}\text{K}_{0.5}\text{Fe}_2\text{As}_2$ single-crystalline microbridges. A crossover temperature T^* was observed in the temperature dependency of the longitudinal resistivity $\rho_{xx}(T)$, which separates $\rho_{xx}(T)$ into temperature-linear and temperature-nonlinear regions. Above T^* , the carriers in $\text{Ba}_{0.5}\text{K}_{0.5}\text{Fe}_2\text{As}_2$ and Co-doped $\text{Ba}_{0.5}\text{K}_{0.5}\text{Fe}_{1.94}\text{Co}_{0.06}\text{As}_2$ demonstrate electronlike behavior and an anomalous nonlinear magnetic field dependence of the Hall voltage with a sign reversal. By contrast, the Zn-doped $\text{Ba}_{0.5}\text{K}_{0.5}\text{Fe}_{1.94}\text{Zn}_{0.06}\text{As}_2$ behaves like a hole type and the Hall coefficient is independent of the magnetic field. The field-induced sign reversal of the Hall coefficient of undoped and Co-doped samples depends on the field modification on the mobility and hole/electron concentration ratio. The T^2 -dependent Hall angle of a nonmagnetic Zn-doped crystal is observed as a nearly parallel shift from that of the impurity-free crystal in the low-temperature region, indicating that the Zn induces a weak change of the spinon excitations, while increasing the number of scattering centers. The Co works as a nonmagnetic impurity as well, while it provides both spinon excitations and impurity scattering.

DOI: [10.1103/PhysRevB.90.024512](https://doi.org/10.1103/PhysRevB.90.024512)

PACS number(s): 74.70.Xa, 74.20.Rp, 74.25.F-, 74.78.Na

I. INTRODUCTION

In the Fe-based superconductors, five $3d$ bands contribute to the Fermi surface, resulting in a rather complicated multiband structure [1–3]. Angle-resolved photoemission spectroscopy (ARPES) confirmed the topology of the Fermi surface as three small hole pockets around the $\Gamma = (0, 0)$ point and two electron pockets around the $\mathbf{M} = (\pi, \pi)$ point in the two-Fe Brillouin zones [4,5]. Therefore, it is crucial to compare the hole and the electron doping cases. Recent optical spectroscopy also revealed two Drude terms in the conductance for optimally doped $(\text{Ba,K})\text{Fe}_2\text{As}_2$ [6], suggesting two types of carriers with different scattering rates. The coexistence of hole and electron carriers is also observed in both p -type and n -type cuprate superconductors [7–9]. Referring to the comprehensive studies on the cuprates, the temperature and magnetic field dependencies of the Hall coefficient are essential probes to elucidate the carrier nature. For the p -type cuprates, for instance, the electron carriers' dominated state is hidden below T_c , and high magnetic fields are therefore necessary to suppress superconductivity and to uncover the normal carrier properties [7,8]. The Hall sign reversal may reflect the reconstruction of the Fermi-surface topology, for example, due to the Lifshitz transition [7]. Such a transition has been recently found in various Fe-based superconductors, such as

the 122-type $(\text{Ba,K})\text{Fe}_2\text{As}_2$ [1] and 11-type $\text{Fe}(\text{Se}_{0.5}\text{Te}_{0.5})$ [2], via normal-state Hall measurements. However, it is difficult to elucidate the picture of electronic state directly from the Hall coefficient data due to the complex character of temperature and field dependencies. Even more, the upper critical field ($H_{c2} \sim 80$ T) is too high to suppress superconductivity due to the nature of charge carriers below the T_c [10].

To solve this problem, in-plane impurity doping, which can adjust the carriers and suppress the superconductivity, is a promising method. Anderson [11] proposed a temperature dependence for the Hall angle ($\cot\Theta_H = \rho_{xx}/\rho_{xy}$, where ρ_{xx} and ρ_{xy} are the longitudinal and transversal resistivity, respectively) from the framework of the Luttinger-liquid theory as a square law $\cot\Theta_H = \alpha T^2 + C$, where α is a parameter representing the energy scale of the spinon-spinon scattering. Here, $\alpha = m_s/eHW_s$, where m_s and W_s are effective mass and the bandwidth of spin excitations, respectively. C is the in-plane impurity contributed scattering rate, being inversely proportional to the impurity contribution τ_M as $C = m_s/eH\tau_M$ [12–14]. Therefore, $\cot\Theta_H$ depends only on the transverse scattering lifetime τ_H , which is determined mainly by spinon-spinon interactions. It has a characteristic T^2 dependence. The appealing features of this theory are that only a few parameters are required to describe the normal-state transport, and that the understanding of the general features of the normal-state properties does not involve the details of the electronic structure. In the cuprate superconductors, for instance YBCO, the parameter C depends linearly on the Zn-doping level x , and α is constant for all doping levels [12].

*Jun.Li@fys.kuleuven.be

†Victor.Moshchalkov@fys.kuleuven.be

As a result, the slopes of $\cot\Theta_H$ are T^2 dependencies for various crystals that are almost constant regardless of the Zn concentration.

For iron-based superconductors, there are only a few reports on the Hall effect measurements for impurity-doped single crystals, i.e., only for the n -type $\text{Ba}(\text{Fe},\text{Co})_2\text{As}_2$ [15] and the p -type $(\text{Ba},\text{K})\text{Fe}_2\text{As}_2$ [16]. The key reason is the technical difficulty to synthesize high-quality impurity-doped single crystals, particularly for the case of high-volatility Zn impurities [17,18]. In addition, it is worth noting that the previous Hall experiments were implemented on bulk crystals [1,2,15,16], where the Hall resistance was generally rather small due to the bulk geometry and the metallic behavior with high carrier densities. To avoid these problems, we used micro- and nanopatterning of superconducting thin films or single crystals cleaved into thin pieces to enhance the Hall signal and to improve the experimental accuracy. Since thin films often possess a high density of microtwins or low-angle grain boundaries [19,20], single crystals are much better suited to obtain intrinsic transport properties, especially in the superconducting state. Recently, we developed a method to fabricate microbridges of single crystals [21]. The thickness of the crystal can be down to 18 nm, thus the in-plane resistance can be as high as $100\ \Omega$ at room temperature, which provides an easy way to study the transport properties of the metallic Fe-based superconductors. On the other hand, the ion beam treatment can often introduce chemical and thermal instability, for instance for the cuprates' superconductors [19]. For the iron-based crystals, however, the superconductivity and normal-state resistivity seem to be strongly against the ion milling, even for the crystal remaining at a few superconducting layers (18 nm) [21].

In the present work, we fabricated microbridges, with a thickness of a few hundreds of nanometers, from high-quality single crystals doped with Zn and Co impurities. On these microbridges, we measured the normal-state Hall coefficient and the angle. The impurity-free $\text{Ba}_{0.5}\text{K}_{0.5}\text{Fe}_2\text{As}_2$ superconductors demonstrate Hall sign reversal above 250 K. Substitution of Co enhances the negative Hall signal at high temperatures, while Zn suppresses this phenomenon. The Hall angle data indicate that the Zn impurities induce in-plane scattering centers but alter the intrinsic relaxation rate via elementary excitations (spinons) only weakly. The Co, however, enhances both scattering and spin excitations.

II. EXPERIMENT

The synthesis method for $\text{Ba}_{0.5}\text{K}_{0.5}(\text{Fe},\text{M})_2\text{As}_2$ ($M = \text{Fe}$, Zn, and Co) single crystals was described elsewhere [15]. This time, we further improved the high-pressure synthesis technique for high-quality single crystals, i.e., the samples were kept at $1300\ \text{°C}$ for 4 hours, and then slowly cooled down to $1100\ \text{°C}$ for 2 hours before quenching to room temperature. In this process, the impurity ions (Zn and Co) can be homogeneously distributed within the superconducting Fe_2As_2 layers to avoid the disorder effects. Here, we focus on three crystals, namely the impurity-free $\text{Ba}_{0.5}\text{K}_{0.5}\text{Fe}_2\text{As}_2$, Zn-doped $\text{Ba}_{0.5}\text{K}_{0.5}\text{Fe}_{1.94}\text{Zn}_{0.06}\text{As}_2$, and Co-doped $(\text{Ba}_{0.5}\text{K}_{0.5}\text{Fe}_{1.94}\text{Co}_{0.06}\text{As}_2)$. We abbreviate them as BK, BKZn, and BKCo, respectively. The contents of Zn and Co

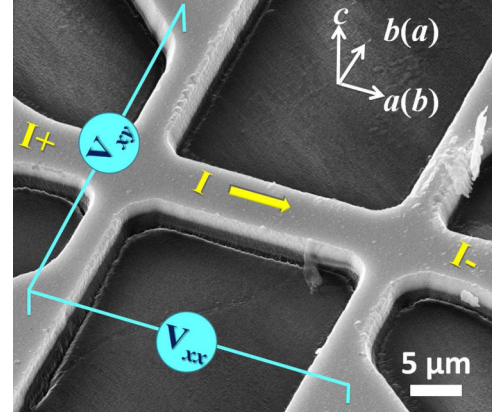


FIG. 1. (Color online) A SEM image of a typical microbridge. The magnetic field was initially applied along the c axis, then the sample was rotated along the axis of longitudinal current I_{xx} . Thus, the effective magnetic fields can be adjusted and the change of Lorentz force can be avoided as well.

were confirmed from energy-dispersive x-ray experiments. The fabrication of the microbridges was introduced in a recent work [21]. In the present work, the microbridges have the width W of $2\ \mu\text{m}$, the length L of $10\ \mu\text{m}$, and thicknesses of 140, 500, and 200 nm for BK, BKZn, and BKCo, respectively. The thickness was determined via ρ_{xx} measurements at room temperature.

The temperature-dependent ρ_{xx} and ρ_{xy} was measured in the Physical Properties Measurement System $-9\ \text{T}$ (Quantum Design). Figure 1 shows a scanning electron microscopy (SEM) image for a typical microbridge. In the measurements, the magnetic field was initially applied along the c axis, and then the sample was rotated along the axis of the applied longitudinal ac current I_{xx} . Thus, the Lorentz force was kept constant with $H(I_{xx}) = 0$. To change the sign of the magnetic field for the Hall coefficient measurements, the sample was rotated along the direction of I_{xx} , thus the effective magnetic field is $H = H_0 \sin[H(I_{xy})]$, where H_0 is the applied field and I_{xy} is the transverse current, i.e., the Hall current. To avoid a magnetoresistance contribution while using the transverse electrodes, we calculated R_{xy} by changing the sign of the field as $R_{xy}(H) = [R_{xy}(H^+) - R_{xy}(H^-)]/2$.

III. RESULTS AND DISCUSSIONS

A. Normal-state resistivity

Figure 2 shows the temperature dependencies of ρ_{xx} for BK, BKZn, and BKCo. The values of ρ_{xx} are about one order of magnitude less than our previous results obtained on bulk crystals [16], suggesting the release of scattering from impurities or other imperfections, which we attribute to the improvement of the crystal synthesis technique. Moreover, in the traditional four-probe measurement technique, a high current bias is often necessary to enhance the measurement resolution, especially for the Hall signal, owing to the specific geometry and strongly metallic behavior of the crystals. In this case, heating can be quite substantial, particularly at the interface between silver paste contact and the crystal. For the present measurement setup, however, the resistance

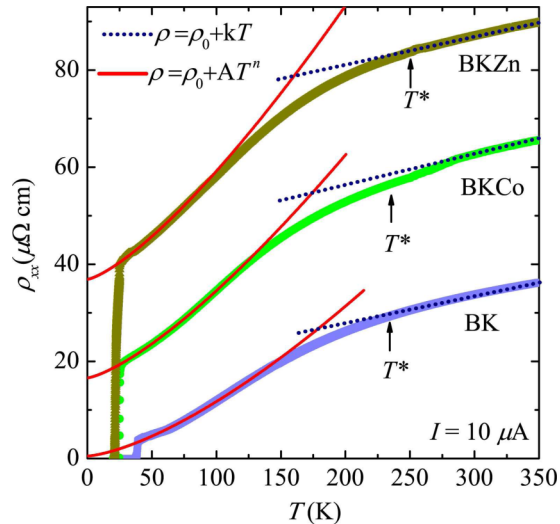


FIG. 2. (Color online) Temperature dependencies of ρ_{xx} for BK, BKZn, and BKCo. The blue dotted lines indicate the T -linear fitting for $\rho(T)$ as $\rho(T) = \rho_0 + kT$, and the red lines correspond to the T -nonlinear $\rho(T)$ fitting as $\rho(T) = \rho_0 + AT^n$. The fitting parameters are given in Table I.

of the microbridge is large enough, normally above 20Ω [21], to apply a current as low as $10 \mu\text{A}$. Moreover, we evaporated a layer of Au and heat treated it at 300°C for 24 hours, so that the interface contact resistance is less than 0.1Ω at room temperature. In particular, the electrodes are superconducting as well (see Fig. 1), thus we can eliminate the heat effects considerably. In addition, in the present measurements, we carefully selected a high-quality area of the crystal with small dimensions of $10 \times 2 \times 0.2 \mu\text{m}^3$.

At temperatures far above T_c , ρ_{xx} shows a linear change with temperature, establishing a metalliclike resistivity dominated by phonons. By contrast, in the low- T region, an obvious superlinear temperature dependence is observed in $\rho_{xx}(T)$, differing from other 122 systems such as the electron-doped $\text{Ba}(\text{Fe},\text{Co})_2\text{As}_2$ [22], the isovalent-doped $\text{Ba}(\text{Fe},\text{Ru})_2\text{As}_2$ [23], and $\text{BaFe}_2(\text{As},\text{P})_2$ [24], for which the $\rho_{xx}(T)$ curves are linear for the entire normal state due to the electron dominated carriers. We fit the superlinear regime using the power law $\rho(T) = \rho_0 + AT^n$ ($n > 1$) as shown by red lines in Fig. 2. Here, ρ_0 is the residual resistivity at 0 K, and the fitting parameters (ρ_0, n) are given in Table I. For the impurity-free sample, $\rho_0 = 0.51 \mu\Omega \text{ cm}$ and $n = 1.46$ are consistent with a recent work [1], for which the power-law fitting on the low T $\rho(T)$ also indicates small powers for both under- and optimal-doped cases, for instance, $n = 1.47$ and 1.62 for $\text{Ba}_{0.45}\text{K}_{0.55}\text{Fe}_2\text{As}_2$ and $\text{Ba}_{0.74}\text{K}_{0.26}\text{Fe}_2\text{As}_2$, respectively. However, all powers are considerably smaller than those for a normal Fermi liquid ($n = 2$) which is dominated by strong electron-electron interactions, probably suggesting an effect from critical antiferromagnetic fluctuations. We should note that since all fittings were based on the normal-state results, it is impossible to deduce the quantum critical profile from the extrapolation of normal state $\rho(T)$ to low T , unless the superconductivity can be suppressed by a high magnetic field [7,8]. Indeed, a slight upturn was observed below T_c by applying fields up

TABLE I. The fitting parameters for T -linear $\rho(T) = \rho_0 + kT$ and T -nonlinear $\rho(T) = \rho_0 + AT^n$ curves as indicated in Fig. 2, and also for $\rho(T) = \rho_0 + BT \exp(-\Delta/T)$ for comparison.

	Parameters	BK	BKZn	BKCo
$\rho(T) = \rho_0 + kT$	ρ_0 ($\mu\Omega \text{ cm}$)	15.78	68.09	35.78
	k ($\mu\Omega \text{ cm K}^{-1}$)	0.06	0.06	0.09
$\rho(T) = \rho_0 + AT^n$	ρ_0 ($\mu\Omega \text{ cm}$)	0.51	36.9	16.7
	A	0.014	0.047	0.035
	n	1.46	1.34	1.36
$\rho(T) = \rho_0 + BT \exp(-\Delta/T)$	ρ_0 ($\mu\Omega \text{ cm}$)	3.00	39.04	19.64
	B ($\mu\Omega \text{ cm K}^{-1}$)	0.24	0.28	0.28
	Δ (K)	98.56	37.00	64.11

to 45 T [10]; due to the high upper critical field ($\sim 90 \text{ T}$), a further increase of field would be essential to obtain clearer results. More importantly, the low quality of the early single crystals should be taken into account for analyzing such an upturn because the crystalline defects often induce disorder and localization. Alternatively, impurity substitution in the superconducting layers is a promising method to uncover the normal state $\rho(T)$ at low T . Our preliminary study demonstrated that substitution of both Zn and Co ions into the Fe site can induce scattering and T_c suppression [15,16]. Particularly, a heavy level of impurity caused a low- T upturn. However, the existence of disorder and localization around the Zn ions should be taken into account for the case of heavy doping. In the present work, the single crystals, regardless of impurity doping or not, are observed to have considerably less normal-state resistivity than our previous one, indicating the improvement of the crystal quality. Here, we investigate the low doping level (3 at.%) of Zn and Co for a comprehensive study of the transport properties, due to the high quality of the single crystals with less disorder or localization. The $\rho(T)$ powers for BKZn and BKCo are estimated as 1.34 and 1.36, respectively, indicating the non-Fermi-liquid behavior for the low- T region as well.

According to our previous expectation, the Co might act as a magnetic impurity within the Fe-based superconductors. In this case, we should obtain negative magnetoresistance due to the Kondo effect [25]. In Fig. 3, we show the magnetoresistivity $\rho_{xx}(H)$ of BKZn and BKCo, where the pulsed magnetic field was up to 45 T and applied along the c axis. The $\rho_{xx}(H)$ of both BKZn and BKCo exhibit a monotonous increase with respect to magnetic fields obeying the Kohler's rule [26], but not the negative magnetoresistance for both Zn- and Co-doped crystals, suggesting that Zn and Co work as nonmagnetic impurities.

The crossover temperatures T^* between the T -linear and T -nonlinear $\rho_{xx}(T)$ are far above T_c . Since BK is in an optimal-doped state, neither the antiferromagnetic transition at a temperature T_N nor a spin-density-wave temperature T_S can be associated with T^* . A pseudogap might be considered as a likely candidate for the crossover at T^* . The evidence for a pseudogap was found from in-plane optical conductivity data obtained on under-doped $\text{Ba}_{1-x}\text{K}_x\text{Fe}_2\text{As}_2$ [6]; this gap was observed at temperature between T_S and T_c , which is different from the pseudogap in cuprate superconductors.

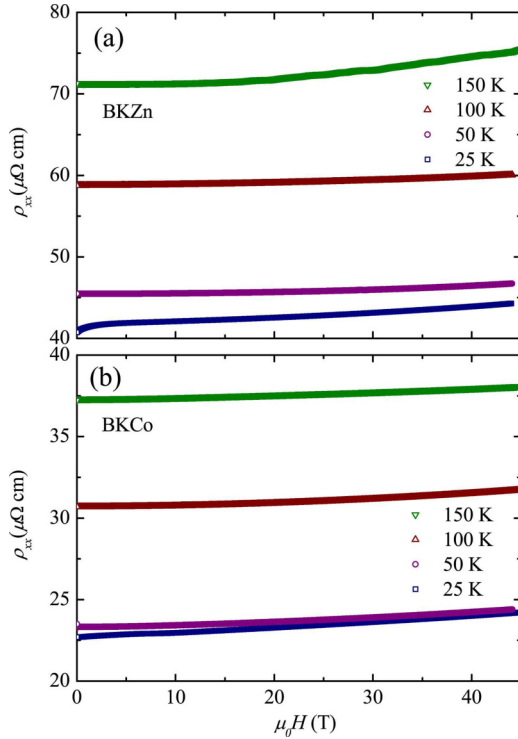


FIG. 3. (Color online) Magnetoresistivity $\rho_{xx}(H)$ for (a) BKZn and (b) BKCo. The pulsed magnetic field was up to 45 T, and applied along the c axis.

For instance, $\rho(T)$ curves of $\text{YBa}_2\text{Cu}_3\text{O}_x$ demonstrate three different regimes defined as (i) T -linear regime above the pseudogap crossover temperature T_p , (ii) T -nonlinear regime between T_p and the Mott-insulator transition temperature T_M , and (iii) Mott-insulator behavior below T_M . Moshchalkov *et al.* [27] proposed a one- or two-dimensional Heisenberg model for the quantum transport in the anisotropic cuprate system. According to the model, $\rho(T)$ can be described by a super-linear T dependence as $\rho(T) = \rho_0 + BT \exp(-\Delta/T)$, where B is a system-dependent constant and Δ is the spin gap arising from spin fluctuations. We also fit the data using this model, and the corresponding fitting parameters are given in Table I.

B. Hall coefficient

Figure 4 shows the field-dependent ρ_{xy} for BK, BKZn, and BKCo at some selected temperatures from 50 to 350 K. For BK, ρ_{xy} shows a linear increase with field at low temperatures, while it becomes nonlinear at high temperatures with $T \geq 250$ K. We define the crossover temperature between the two regimes as T_H . Surprisingly, T_H is well in accordance with the T^* , as shown in Fig. 2. However, the nonlinearity is present only below fields of ~ 3 T, which seems to be a saturation field for the $\rho_{xy}(H)$ dependence to be linear. Note that an obviously negative ρ_{xy} is observed at $T = 300$ K, while the negative signal tends to weaken as T approaches 350 K. Applying substitution of Zn impurities, the Hall resistivity ρ_H of the BKZn is linear and remains positive for fields up to 7 T. On the contrary, the Co impurities substitution reinforces the nonlinear and negative behavior of $\rho_{xy}(H)$, which can be seen in fields up to 7 T.

Figure 5 presents contour plots of R_H for BK, BKZn, and BKCo as a function of magnetic field and temperature. For BK, $R_H(H)$ shows two pronounced regions, namely an H -dependent region above 240 K and an H -independent region below ~ 240 K as described above. In the H -independent region, R_H is positive, indicating hole-type carriers. In the H -dependent region, $R_H(H)$ is negative at relatively low fields, indicating that electrons are the dominant carriers. However, further increasing the field turns the Hall sign back to positive, suggesting the presence of hole-type carriers. By introducing Zn ions into BK, at low temperature, R_H is increased to about twice the value for BK. The field dependence is modified as well, i.e., R_H is independent of field in the whole temperatures region and it is always positive. For the Co impurities substituted in BK, R_H is more complicated: (i) There is a pronounced increase of R_H from the undoped crystal. (ii) It has strongly H -dependent behavior at high temperature, and T_H (~ 240 K) seems to be independent of Co doping, being of the same value as that of BK. (iii) The negative R_H regime exists in almost the whole H -dependent region, and here a high field (> 7 T) is necessary to suppress the negative R_H . Considering our early results on Zn-doped crystals [15], the Hall coefficient was observed to have a sign reversal, which is

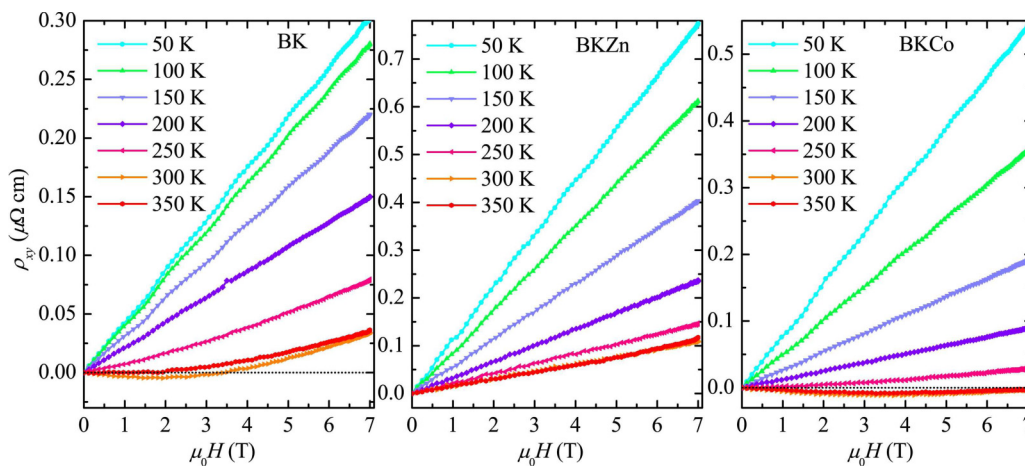


FIG. 4. (Color online) Magnetic field dependence of ρ_{xy} for BK, BKZn, and BKCo; ρ_{xy} was calculated as $\rho_{xy}(H) = [\rho_{xy}(H^+) - \rho_{xy}(H^-)]/2$ from the deviation from longitudinal resistances under positive and negative fields.

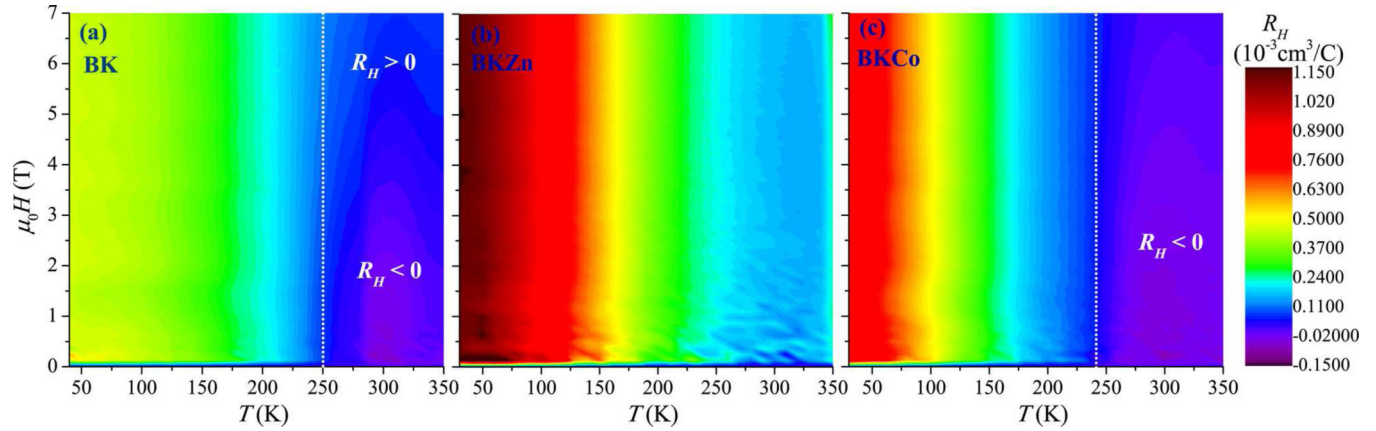


FIG. 5. (Color online) Contour plots of R_H for BK, BKZn, and BKCo as a function of magnetic field and temperatures. The white dotted line separates regions demonstrating field-dependent (right) and field-independent (left) regions for $R_H(H)$.

opposite to the present data. We ascribe the early results to the technique error from the measurement setup. For the present microbridge, the Hall resistance can be up to a few $m\Omega$, which is large enough for accurate measurements.

In order to elucidate the carrier profiles for various temperatures and fields, we calculated from R_H the effective carrier density $n_{\text{eff}} = nV$, where V is the volume per Fe ion and $n = 1/eR_H$ is the carrier density. Figure 6 shows the contours of n_{eff} as a function of T and H for BK, BKZn, and BKCo. The n_{eff} of BK is also separated into H -independent and H -dependent regions. It is independent of the field below T_H , while it depends on H above T_H . Note that there are more than two types of carriers per Fe above T_H , indicating high hole densities. Since there is a crossover field for the sign reversal for the Hall coefficient, it is reasonable to obtain rather small R_H values, as shown in Fig. 5. Thus, we argue that the n_{eff} in this temperature region can hardly reflect the real carrier densities. Below T_H , n_{eff} decreases gradually, down to 0.5 per Fe near T_c . In the case of Zn doping, n_{eff} is H independent at all temperatures. For BKCo, the carriers are the electron type at almost all fields for temperatures above T_H . However, the values of n_{eff} for both BKZn and BKCo are similar to those of BK below T_H , indicating that the impurities induce

modification only in the electron pocket but not in the hole pocket.

The sign reversal of n_{eff} may indicate a crossover involving a Fermi-surface reconstruction. In the Fe-based superconductors, however, the Fermi structure has a rather complicated multiband nature, including three small hole pockets around the $\Gamma = (0, 0)$ point and two electron pockets around the $\mathbf{M} = (\pi, \pi)$ point [3]. The effective carrier concentrations are dominated by the competition between the hole and the electron pockets, and it can be described by a two-band Drude model,

$$n_{\text{eff}} = \frac{(n_h + n_e b)^2}{n_h (1 - r) b^2}, \quad (1)$$

where n_h and n_e are the carrier densities of holes and electrons, $r = n_e/n_h$ is the ratio of carrier densities, and $b = \mu_e/\mu_h$ is the ratio of the electron μ_h and the hole mobility μ_e . Thus, the sign of effective carrier density depends on the hole and electron carrier density and their mobility ratios. The mobility is determined by two physical parameters as

$$\mu = e\tau/m^*. \quad (2)$$

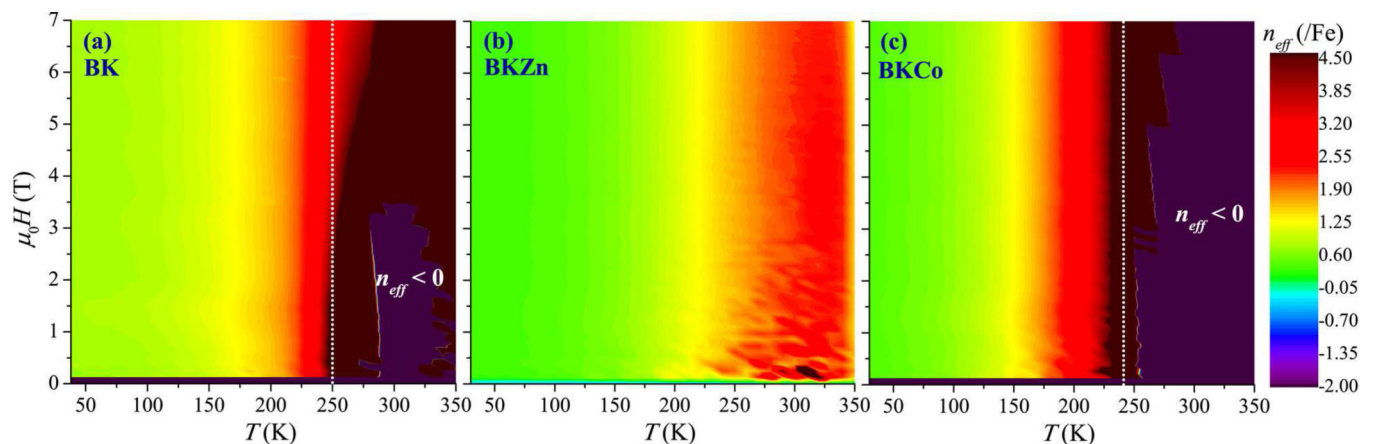


FIG. 6. (Color online) Contours of n_{eff} for BK, BKZn, and BKCo as a function of magnetic field and temperature. The n_{eff} per Fe ion is estimated from $n_{\text{eff}} = nV$, where V is the volume per Fe ion and $n = 1/eR_H$ is the carrier density. The white dotted line separates field-dependent (right) and field-independent (left) regions for $n_{\text{eff}}(H)$.

Here, τ^{-1} is the scattering rate corresponding to the impurity scattering. The hole carriers are generally observed to have significantly larger m^* than electrons, resulting in $b = \mu_e/\mu_h > 1$. Consequently, n_e must be less than n_h for a positive n_{eff} . For a negative n_{eff} , however, n_e can be less or even larger than n_h depending on the mobility ratio.

Here, we propose at least four contributions for the sign of n_{eff} . The first one is the hole-doping level, which determines the n_e and n_h , and consequently the sign of n_{eff} according to Eq. (1). Ohgushi and Kiuchi [1] have comprehensively studied $\text{Ba}_{1-x}\text{K}_x\text{Fe}_2\text{As}_2$ with $0 < x < 0.55$. The electron and hole pockets coexist within the Fermi structure at all doping levels, while the electrons are the dominant carrier species below the quantum critical point at $x = 0.14$. The hole contribution dominates once the doping level is above 0.14. We stress that the electron pocket exists until Ba is completely substituted by K, forming the single-band superconductor KFe_2As_2 .

The second factor is temperature, since both carrier density and mobility are temperature dependent, and electron and hole behave differently with respect to temperature variation. The mobilities of electrons and holes show less difference at high temperatures due to a lower relaxation time. As a result, it is reasonable to obtain a negative n_{eff} for BK at high temperatures, even though n_e is significantly less than n_h in the present optimally doped case. At low temperatures, however, the carriers tend to resist trapping by impurities and scattering from lattice vibrations, resulting in dramatic increase of τ , and, consequently, the mobilities tend to increase regardless if they are hole or electron species. A crossover temperature (T_0) for the electron-hole transition (EHT) was observed for the samples with $x < 0.14$ [1]. T_0 decreases with increasing hole level caused by the particular T dependence of n and μ , which are different for electrons and holes.

Third, the applied magnetic field should be taken into account. Considering the simple Drude model, both carrier density and mobility are H independent; as a result, it is impossible to observe field-induced sign reversal according to Eq. (1). Either carrier density or mobility should depend on the applied field for the sign reversal. For our present result for BK and BKCo, the electron contribution seems to be suppressed by field (~ 3 and ~ 7 T, respectively). As H increases up to 5 T, n_{eff} for BK is H independent at all temperatures and is dominated by holes. Thus, the absence of the previously reported electron-type signal may be due to too high applied magnetic fields (normally 7 T or above). Particularly, the electron-type signal can be suppressed even for strongly electron-doped compounds, once the field is high enough. Huang and co-workers [28] studied the Hall resistivity of the parent compound BaFe_2As_2 and electron-doped $\text{Ba}(\text{Fe},\text{Co})_2\text{As}_2$, both revealing electron-carrier-like $\rho_{xy}(H)$ under relatively low fields, while gradually becoming positive at high magnetic fields up to 55 T. The sign reversal is pronounced at low temperatures below the spin-density-wave (SDW) state, where the electron carriers are considered as two groups, which contribute to the localized moments and transport property, respectively. A similar phenomenon was also found in the cuprates, for instance in the electron-doped $\text{Pr}_{2-x}\text{Ce}_x\text{CuO}_{4-\delta}$ superconductors [9]. It seems likely that electrons are more sensitive to the field than the hole carriers, given that for hole-type superconductors, extremely high

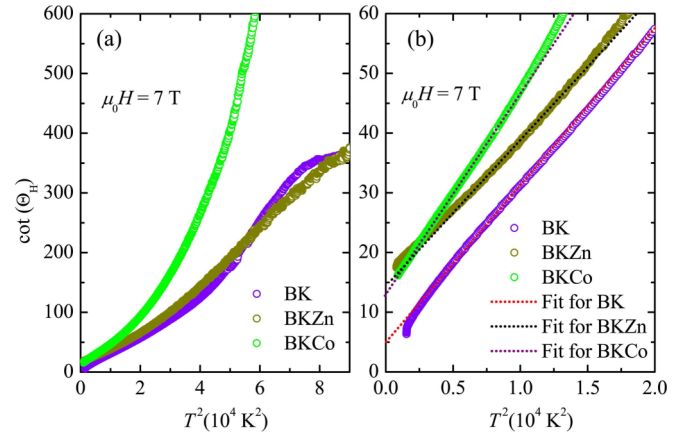


FIG. 7. (Color online) Cotangent of the Hall angle $\cot\Theta_H = \rho_{xx}/\rho_{xy}$ for a systematic set of BK, BKZn, and BKCo samples. The low-temperature data (< 140 K) can be fitted by a square law $\cot\Theta_H = \alpha T^2 + C$ and are given by dotted lines in (b).

magnetic field only weakly alters the carrier profiles, except for temperatures below T_c . LeBoeuf and co-workers [7,8] studied carriers of the hole-doped high- T_c compound YBCO in fields up to 60 T. They discovered a crossover temperature for a hole-electron transition (HET) for superconductors with doping n_h higher than a critical value 0.08, indicating the opposite response for YBCO compared to BK. We stress that a field-induced sign reversal can appear in the mixed state [7–9], where a negative flux-flow voltage can contribute to the Hall signal. Our preliminary pulsed high field (52 T) experiments on BK, BKZn, and BKCo reveal that the carriers are holelike and H independent below T_c , which will be addressed in a separate future study.

The last but not the least factor is the impurity doping. Substitution of impurity on the Fe site induces reorganization of the electronic structure and, as a result, alters the electron carrier density. In our present study, the Co doping enhances the electron-type Hall signal at high temperatures, which also supports our understanding of the electronlike Hall behavior of BK. On the other hand, since the hole-doping level is constant ($x \equiv 0.5$) regardless of impurity concentration, the hole carrier density should be independent of impurities. For the Zn-substituted BK, the electronlike Hall signal completely disappears. Although the Zn ion supplies four additional $3d$ electrons to Fe, it does not seem to enhance the electron carrier density. To investigate the possible effect of Zn^{2+} on the electronic state, we studied the Hall angle for both impurity-free and impurity-doped samples.

C. Hall angle

Figure 7(a) shows the T^2 dependence of the cotangent of the Hall angle $\cot\Theta_H$ for BK, BKZn, and BKCo. All curves reveal a nonlinear change with T^2 at the high- T region. For the BK, for instance, the nonlinear T^2 dependence appears above 240 K, suggesting a larger power of T^n with $n > 2$. The crossover temperature, however, is well in accordance with both T^* and T_H , as discussed above. For nonmagnetic Zn substitution, $\cot\Theta_H$ shows a weakly nonlinear variation at high T . For the nonmagnetic Co impurity, however, $\cot\Theta_H(T^2)$

indicates a dramatic modification from BK at high T . Since the Hall signals are rather small in this temperature region, where sign reversal happens as discussed above, we can hardly extract trustworthy information from this data. Below, we focus on the low- T regions, where $\cot\Theta_H$ changes linearly with T^2 . Figure 7(b) gives the linear fitting of T^2 for $\cot\Theta_H$ of BK, BKZn, and BKCo at $T < 140$ K ($\cot\Theta_H = \alpha T^2 + C$). The parameters $\alpha(C)$ are found to be $2.69 \times 10^{-3} \text{ K}^{-2}$ (3.96), $2.43 \times 10^{-3} \text{ K}^{-2}$ (15.38), and $3.48 \times 10^{-3} \text{ K}^{-2}$ (12.84) for BK, BKZn, and BKCo, respectively. Adding Zn does not seem to change the slope of $\cot\Theta_H$ from that of BK. Anderson proposed an explanation for this phenomenon based on the Luttinger-liquid theory. The behavior of $\cot\Theta_H$ is consistent with the intrinsic relaxation rate of the elementary excitations (spinons) in the normal state, but not with the longitudinal relaxation rate. Indeed, the weak modification of the spin state due to Zn doping was confirmed by the ^{75}As nuclear magnetic resonance (NMR) and nuclear quadrupole resonance (NQR) measurements on $\text{LaFe}_{1-x}\text{Zn}_x\text{AsO}_{0.85}$ polycrystals [29]. The ^{139}La NMR spectra also indicated that the substituted Zn could hardly induce static moments around the impurity [29]. On the other hand, the Zn substitution substantially increases the in-plane impurity scattering rate C (15.38) from that of BK (3.96). This is reasonable because the Zn provides a large negative scattering potential (around -8 eV [30]) within the Fe_2As_2 plane. Indeed, our previous study showed that Zn increases the residual resistivity in a linear way and, consequently, suppresses the superconductivity [16]. Substitution of Zn in YBCO leads to a similar parallel shift of the $\cot\Theta_H$ vs T^2 curves with different doping levels [12].

For the case of Co impurity, it increases both α and C . Substitution of Co in the YBCO superconductors also results in a pronounced increase of α , which was attributed to the decrease of the hole concentration. Although our effective Hall carrier data demonstrated a reduction of the hole concentration, Co impurities alter both the hole and the electron pockets due to the multiband Fermi structure. Considering spin fluctuations, the present pnictide superconductors exhibit a more complex profile than the cuprates. We argue that the effects of Co on the slope of $\cot\Theta_H$ vs T^2 can hardly be explained by variation of either hole numbers or spin excitations alone. On the other hand, C is almost independent of doping in the YBCO case, due to the weak change of the residual resistivity. In that case, Co was considered as an out-of-plane (the CuO plane) rather than an in-plane (the CuO_2 plane) scattering center. In the Fe-based superconductors, however, a pronounced increase of the residual resistivity is observed, as can be seen from Fig. 1, and the residual resistivity also exhibits a linear increase with the Co-doping level, as described

in our previous study [15]. As a result, the C value in BKCo is also increased. In addition, Cheng and co-workers' [31] study on the Fe and As K edge of $\text{Ba}_{0.5}\text{K}_{0.5}\text{Fe}_2\text{As}_2$, using the extended x-ray absorption fine-structure spectroscopy, and the Zn impurities were found to modify FeAs_4 tetrahedron weakly, while the magnetic Mn was observed to cause a gradual deviation of the symmetric FeAs_4 tetrahedron and FeAs bond weakening. Similar results were reported on the Ru-doped $\text{SmFe}_{1-x}\text{Ru}_x\text{AsO}_{0.85}\text{F}_{0.15}$ system [32]. The local structural modification due to different impurities may also contribute to the scattering as well as the superconductivity, thus further study on the local structure is demanded.

IV. CONCLUSIONS

In summary, we fabricated Zn and Co impurity-doped $\text{Ba}_{0.5}\text{K}_{0.5}\text{Fe}_2\text{As}_2$ single-crystalline microbridges with thickness of a few hundred nanometers. The longitudinal resistivity exhibited a crossover temperature T^* separating a T -linear from a T -nonlinear region above and below T^* . Magnetoresistivity of Zn- and Co-doped crystals showed a monotonous increase with respect to magnetic fields obeying the Kohler's rule, indicating that Zn and Co work as nonmagnetic impurities. The Hall resistivity of $\text{Ba}_{0.5}\text{K}_{0.5}\text{Fe}_2\text{As}_2$ and Co-doped $\text{Ba}_{0.5}\text{K}_{0.5}\text{Fe}_{1.94}\text{Co}_{0.06}\text{As}_2$ is demonstrated to be nonlinear in the field change above the crossover temperature, and the sign of the Hall coefficient is also changed from negative to positive with increasing field. This effect is absent for the Zn-doped crystal. The sign change of carriers is due to the increase in the hole-electron mobility ratio. A T^2 dependence of the Hall angle of Zn-doped $\text{Ba}_{0.5}\text{K}_{0.5}\text{Fe}_{1.94}\text{Zn}_{0.06}\text{As}_2$ is observed as a nearly parallel shift from that of the impurity-free crystal, indicating that the Zn induces a weak change in the spinon excitations, while enhancing the scattering rates. By contrast, the dopant Co provides both spinon excitations and impurity scattering.

ACKNOWLEDGMENTS

This research was supported by Methusalem Funding by the Flemish government, the EU-FP6-COST Action MP1201, the World Premier International Research Center from MEXT, the Grants-in-Aid for Scientific Research (Grants No. 25289233 and No. 25289108) from JSPS, the Funding Program for World-Leading Innovative R&D on Science and Technology (FIRST Program) from JSPS, and the National Natural Science Foundation of China (Grants No. 11234006 and No. 51102188).

[1] K. Ohgushi and Y. Kiuchi, *Phys. Rev. B* **85**, 064522 (2012).
 [2] I. Tsukada, M. Hanawa, Seiki Komiya, T. Akiike, R. Tanaka, Y. Imai, and A. Maeda, *Phys. Rev. B* **81**, 054515 (2010).
 [3] J. Paglione and R. L. Greene, *Nat. Phys.* **6**, 645 (2010).
 [4] H. Ding, P. Richard, K. Nakayama, K. Sugawara, T. Arakane, Y. Sekiba, A. Takayama, S. Souma, T. Sato, T. Takahashi, Z. Wang, X. Dai, Z. Fang, G. F. Chen, J. L. Luo, and N. L. Wang, *Europhys. Lett.* **83**, 47001 (2008).

[5] M. P. Allan, A. W. Rost, A. P. Mackenzie, Yang Xie, J. C. Davis, K. Kihou, C. H. Lee, A. Iyo, H. Eisaki, and T.-M. Chuang, *Science* **336**, 563 (2012).
 [6] Y. M. Dai, B. Xu, B. Shen, H. Xiao, H. H. Wen, X. G. Qiu, C. C. Homes, and R. P. S. M. Lobo, *Phys. Rev. Lett.* **111**, 117001 (2013).
 [7] D. LeBoeuf, N. Doiron-Leyraud, B. Vignolle, M. Sutherland, B. J. Ramshaw, J. Levallois, R. Daou, F. Laliberté,

- O. Cyr-Choinière, J. Chang, Y. J. Jo, L. Balicas, R. Liang, D. A. Bonn, W. N. Hardy, C. Proust, and L. Taillefer, *Phys. Rev. B* **83**, 054506 (2011).
- [8] D. LeBoeuf, N. Doiron-Leyraud, J. Levallois, R. Daou, J.-B. Bonnemaïson, N. E. Hussey, L. Balicas, B. J. Ramshaw, R. Liang, D. A. Bonn, W. N. Hardy, S. Adachi, C. Proust, and L. Taillefer, *Nature (London)* **450**, 533 (2007).
- [9] P. Li, F. F. Balakirev, and R. L. Greene, *Phys. Rev. Lett.* **99**, 047003 (2007).
- [10] H. Q. Yuan, J. Singleton, F. F. Balakirev, S. A. Baily, G. F. Chen, J. L. Luo, and N. L. Wang, *Nature (London)* **457**, 565 (2009).
- [11] P. W. Anderson, *Phys. Rev. Lett.* **67**, 2092 (1991).
- [12] T. R. Chien, Z. Z. Wang, and N. P. Ong, *Phys. Rev. Lett.* **67**, 2088 (1991).
- [13] A. Carrington, A. P. Mackenzie, C. T. Lin, and J. R. Cooper, *Phys. Rev. Lett.* **69**, 2855 (1992).
- [14] H. Alloul, J. Bobroff, M. Gabay, and P. J. Hirschfeld, *Rev. Mod. Phys.* **81**, 45 (2009).
- [15] J. Li, Y. F. Guo, S. B. Zhang, J. Yuan, Y. Tsujimoto, X. Wang, C. I. Sathish, Y. Sun, S. Yu, W. Yi, K. Yamaura, E. Takayama-Muromachiu, Y. Shirako, M. Akaogi, and H. Kontani, *Phys. Rev. B* **85**, 214509 (2012).
- [16] J. Li, Y. F. Guo, S. B. Zhang, S. Yu, Y. Tsujimoto, H. Kontani, K. Yamaura, and E. Takayama-Muromachi, *Phys. Rev. B* **84**, 020513(R) (2011).
- [17] B. vom Hedt, W. Lisseck, K. Westerholt, and H. Bach, *Phys. Rev. B* **49**, 9898 (1994).
- [18] Y. F. Guo, Y. G. Shi, S. Yu, A. A. Belik, Y. Matsushita, M. Tanaka, Y. Katsuya, K. Kobayashi, I. Nowik, I. Felner, V. P. S. Awana, K. Yamaura, and E. Takayama-Muromachi, *Phys. Rev. B* **82**, 054506 (2010).
- [19] J. H. Durrell, C.-B. Eom, A. Gurevich, E. E. Hellstrom, C. Tarantini, A. Yamamoto, and D. C. Larbalestier, *Rep. Prog. Phys.* **74**, 124511 (2011).
- [20] H. Hilgenkamp and J. Mannhart, *Rev. Mod. Phys.* **74**, 485 (2002).
- [21] J. Li, J. Yuan, Y.-H. Yuan, J.-Y. Ge, M.-Y. Li, H.-L. Feng, P. J. Pereira, A. Ishii, T. Hatano, A. V. Silhanek, L. F. Chibotaru, J. Vanacken, K. Yamaura, H.-B. Wang, E. Takayama-Muromachi, and V. V. Moshchalkov, *Appl. Phys. Lett.* **103**, 062603 (2013).
- [22] N. Ni, M. E. Tillman, J.-Q. Yan, A. Kracher, S. T. Hannahs, S. L. Bud'ko, and P. C. Canfield, *Phys. Rev. B* **78**, 214515 (2008).
- [23] F. Rullier-Albenque, D. Colson, A. Forget, P. Thuéry, and S. Poissonnet, *Phys. Rev. B* **81**, 224503 (2010).
- [24] S. Jiang, H. Xing, G. Xuan, C. Wang, Z. Ren, C. Feng, J. Dai, Z. Xu, and G. Cao, *J. Phys.: Condens. Matter* **21**, 382203 (2009).
- [25] D. C. Ralph and R. A. Buhrman, *Phys. Rev. Lett.* **69**, 2118 (1992).
- [26] J. M. Harris, Y. F. Yan, P. Matl, N. P. Ong, P. W. Anderson, T. Kimura, and K. Kitazawa, *Phys. Rev. Lett.* **75**, 1391 (1995).
- [27] V. V. Moshchalkov, J. Vanacken, and L. Trappeniers, *Phys. Rev. B* **64**, 214504 (2001).
- [28] H. Q. Yuan, L. Jiao, F. F. Balakirev, J. Singleton, C. Setty, J. P. Hu, T. Shang, L. J. Li, G. H. Cao, Z. A. Xu, B. Shen, and H. H. Wen, [arXiv:1102.5476](https://arxiv.org/abs/1102.5476).
- [29] S. Kitagawa, Y. Nakai, T. Iye, K. Ishida, Y. F. Guo, Y. G. Shi, K. Yamaura, and E. Takayama-Muromachi, *Phys. Rev. B* **83**, 180501(R) (2011).
- [30] K. Nakamura, R. Arita, and H. Ikeda, *Phys. Rev. B* **83**, 144512 (2011).
- [31] J. Cheng, P. Dong, W. Chu, W. Xu, H. Wen, A. Marcelli, and Z. Wu, *J. Synchrotron Radiat.* **20**, 455 (2013).
- [32] L. Simonelli, A. Al-Zein, M. Moretti Sala, B. Joseph, A. Iadecola, M. Bendele, A. Martinelli, A. Palenzona, M. Putti, G. Monaco, and N. L. Saini, *J. Phys.: Condens. Matter* **26**, 065701 (2014).